Pergamon

0028-3908(95)00142-5

Neuropharmacology, Vol. 34, No. 11, pp. 1387–1395, 1995

0028-3908/95 $9.50 + 0.00

Variation in the Number, Location and Size of Synaptic Vesicles Provides an Anatomical Basis for the Nonuniform Probability of Release at Hippocampal CA1 Synapses

K. M. HARRIS* and P. SULTAN

[1]*Department of Neurology, Children's Hospital, Enders 260, 300 Longwood Ave., Boston, MA 02115, U.S.A. and Harvard Medical School*

(Accepted 30 August 1995)

Summary—Synaptic vesicles, synaptic clefts and postsynaptic areas were measured in three dimensional reconstructions at representative axonal boutons in hippocampal area CA1. Both docked and non-docked vesicles were counted and measured. Small boutons on thin spines had about 2–6 docked vesicles from a pool of more than 200 vesicles. Medium-sized boutons on medium-sized mushroom-shaped dendritic spines contained about 13–16 docked vesicles from a pool of more than 450 vesicles. A large bouton synapsing with a large mushroom-shaped dendritic spine had two clusters of vesicles totaling more than 1000 vesicles. The postsynaptic density was segmented into two discrete zones under the two clusters of vesicles and 36 docked vesicles were distributed over its surfaces. Two multiple-synapse boutons contained more than 500 vesicles with 2–12 docked vesicles observed at each of the two postsynaptic densities on each bouton. This nonuniform number of docked vesicles provides an anatomical basis for the non-uniform probability of release that occurs across hippocampal synapses of different sizes. In addition, the volume of each synaptic vesicle was determined to be 0.4–5.2% of the total volume of the reconstructed synaptic clefts into which they presumably release their contents. However, since each vesicle contains more than 10 times the concentration of glutamate needed to saturate the postsynaptic receptors, these data also support the hypothesis that release of even a single synaptic vesicle will activate all of the postsynaptic receptors.

Keywords—Dendritic spines, postsynaptic density, serial electron microscopy, glutamate, dendrites, axons.

The release of neurotransmitter from synaptic vesicles is the first step in the communication between neurons via synaptic transmission. Many recent findings on the molecular mechanisms of synaptic transmission have shown clear evidence that a series of steps constitute the synaptic vesicle (SV) cycle (Sudhof, 1995). These steps involve, (1) docking and (2) priming of SVs prior to (3) fusion and exocytosis of their contents, (4) endocytosis of the SV membrane, probably by way of the clathrin-coated pits, (5) translocation of the coated vesicles to the interior of the axonal bouton, during which they shed their coats and acidify the interior of the recycling vesicle, (6) fusion of the recycling vesicles with endosomes, (7) budding of new vesicles from the endosomes, (8) accumulation of neurotransmitter into the vesicles, and (9) translocation of the SVs back to the active zone. This SV cycle requires about 1 min to complete (Betz and Bewick, 1992; Ryan *et al.*, 1993), and alterations in any of these steps can result in short or long-lasting changes in synaptic efficacy (Sudhof, 1995).

Many components of the SV cycle also have distinct anatomical signatures (Heuser and Reese, 1973; Schwartz, 1992; Peters *et al.*, 1991). Here we highlight those signatures occurring at excitatory synapses in the central nervous system in hippocampal area CA1. The docking and priming of SVs is signified by an SV located immediately adjacent to the active zone across from a postsynaptic density (PSD). Fusion and exocytosis are occasionally captured as 'omega' figures, however, it is not possible to be certain whether these profiles represent SVs that are releasing their contents or are in the process of re-uptake. Endocytosis also occurs via coated pits and vesicles and subsequent recycling of vesicles involves

*To whom correspondence should be addressed, at: Department of Neurology, Children's Hospital, Enders 260, 300 Longwood Ave. Boston, MA 02115, Phone: 617-355-6373, Fax: 617-738-1542

endosomes, which are larger cisterns or tubular structures that are surrounded by a smooth membrane. The large pool of non-docked vesicles is where steps 8 and 9 probably occur.

Recent models and experimental evidence suggest that the glutamate contained within a hippocampal synaptic vesicle could saturate the postsynaptic receptors upon release into the synaptic cleft (Clements *et al.*, 1992; Rosenmund *et al.*, 1993). Physiological evidence also suggests that the probability of release is low at hippocampal synapses but is likely to increase in proportion to the number of readily releasable vesicles (Hessler *et al.*, 1993; Rosenmund *et al.*, 1993). To determine whether postsynaptic receptor saturation could occur for a particular vesicle or set of vesicles, several features must be discerned. The volume and concentration of neurotransmitter in each vesicle will determine how much is available for release. If only part of the vesicle is released, then the amount in the cleft will be less. The concentration of neurotransmitter in the cleft could also be affected by the volume of the cleft and how many vesicles are simultaneously released during an event. This final concentration will be modified with time by diffusion into the surrounding extracellular space and/or re-uptake either into the presynaptic bouton or adjacent astrocytic processes.

Serial electron microscopy (EM) was used to reconstruct entire presynaptic axonal boutons, to measure the volumes of the synaptic vesicles they contain, and to discern the size, number and location of anatomically docked vesicles for each synapse on the bouton. Similarly, the volume of the synaptic clefts, into which the vesicles release their contents, was measured through serial EM. Through these measurements we provide an anatomical basis for the variation in probability of release across hippocampal synapses, and arrive at a range in the percent reduction in neurotransmitter concentration that is likely to occur in synaptic clefts during single synaptic events at hippocampal CA1 synapses.

METHODS

Tissue preparation and electron microscopy

In earlier work (Harris and Stevens, 1989), an adult male rat of the Long–Evans strain (310 g) was perfused through the heart under deep pentobarbital anesthesia with 2% paraformaldehyde, 2.5% glutaraldehyde, 2 mM $CaCl_2$ in 0.1 M cacodylate buffer at pH 7.35, 37°C and 4 psi. The brain was left undisturbed in the cranium for 1 hr and then the hippocampus was removed and sliced at 400 μm thickness. These slices were washed in buffer (0.1 M Cacodylate), soaked for 1 hr in 1% OsO_4 with 1.5% potassium ferrocyanide, and an additional 1 hr in 1% OsO_4. Then the slices were rinsed in buffer, 30 and 50% ethanol, soaked for 1 hr in 1% uranyl acetate in 70% ethanol, dehydrated through graded ethanols to 100% ethanol, propylene oxide, embedded in Epon, and serially thin sectioned on a Reichardt Ultracut E ultramicrotome at silver (later determined to be $\sim$0.055 μm by the section thickness formula described in Harris and Stevens, 1989). The sections were mounted on Formvar-coated slot grids (Synaptek), stained for 5 min with Reynolds' lead citrate, placed in a grid cassette, and stored in numbered gelatin capsules. The grid cassettes were mounted in a rotating stage and a region located approx 200 μm from the pyramidal cell body was photographed on the JEOL 1200EX transmission electron microscope, through 89 serial sections at a consistent orientation, along with a calibration grid (0.463 μm per square, Pella). From this series, seven axonal boutons and their associated synaptic components were chosen for 3-D reconstruction. These boutons were chosen to represent the broad range in size and type of postsynaptic partners found in s. radiatum. In addition, each the synaptic junctions had to be sectioned across the PSD to reveal the synaptic cleft between the bouton and its postsynaptic partner(s) and enable us to obtain accurate measurements of its dimensions across serial sections. When the reconstructions were complete, we compared the sizes of the PSDs, total number of synaptic vesicles, and dimensions of the spines and boutons to the larger populations from our previous studies, thereby confirming that these seven boutons and synaptic complexes were comparable to the larger population.

RESULTS

Ultrastructural characteristics of the synaptic components

Figure 1 illustrates the components of the synapses that were analyzed. Non-docked vesicles were located in the center of the bouton and their perimeters were traced when a distinct membrane was visible around the vesicle [Fig. 1(A)]. Docked vesicles were located immediately across from the postsynaptic density (PSD) on the spine head and were completely apposed to the presynaptic membrane such that no axoplasm was visible between the adjacent membranes [Fig. 1(B, E, G) curved arrows]. Coated pits [e.g. Fig. 1(G)] or vesicles (not shown) were observed in some boutons on the side of the axon membrane away from the spine head and PSD. The synaptic clefts were defined by the space between the pre- and postsynaptic membranes that was filled with dense-staining material [Fig. 1(C)]. The extracellular space was defined as the region between the axonal and spine membranes not containing dense-staining material [Fig. 1(F)]. Each of these structures was traced completely through serial sections. Dendritic spines were capped by the gray profiles of their plasma membranes [Fig. 1(H)].

Three-dimensional reconstructions

Axonal boutons and their associated postsynaptic partners were traced and measured through serial sections using the V8 system of programs developed in the Image

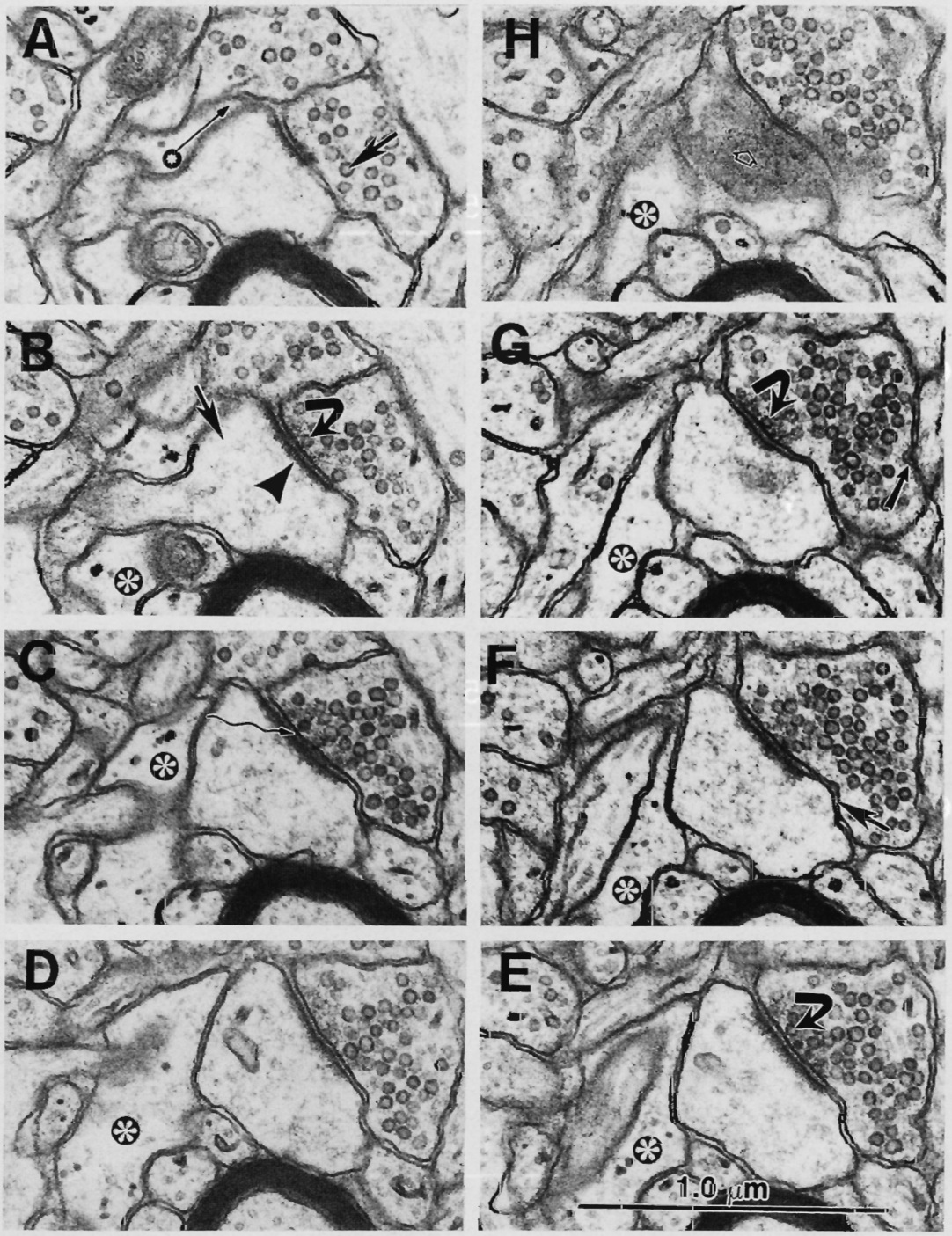

Fig. 1. Serial electron micrographs through a macular postsynaptic density on a mushroom-shaped dendritic spine. Each of the eight micrographs contains a section through the dendritic spine and its corresponding presynaptic bouton. (A) A characteristic non-docked vesicle (arrow) in the presynaptic bouton. (B) A characteristic docked vesicle (curved arrow), across from the postsynaptic density (PSD, arrow head); on the spine head (arrow). (C) The synaptic cleft (wiggly arrow) is the region between the plasma membranes of the dendritic spine head and the presynaptic axonal bouton that contains dense staining material. (D) Serial section with C and E. (E) Curved arrow illustrates another typical docked vesicle. (F) Extracellular space (arrow) is region between the spine and the bouton that does not contain dense-staining material. (G) Docked vesicle (curved arrow) near the PSD and coated pit (straight arrow) on other side of the bouton. (H) Gray edge of the plasma membrane (open arrow) capping the head of the dendritic spine. In all sections, part of an astrocytic process (*) can be identified to surround the spine neck and part of the spine head and a finger-like projection [* with long arrow in Fig. 1(A)] occurs in the extracellular space adjacent to the synapse.

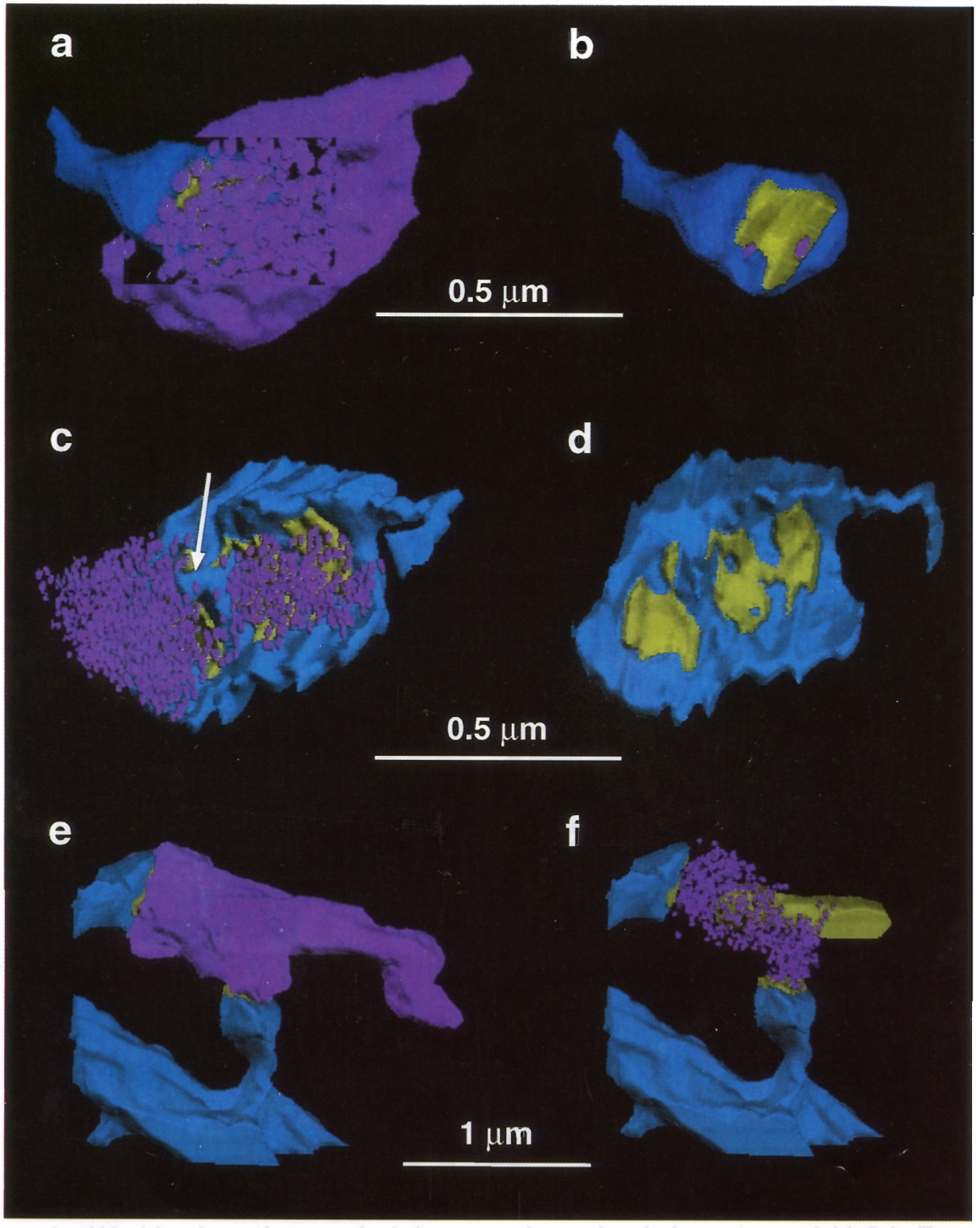

Fig. 2. Reconstructions of presynaptic boutons containing vesicles (purple), dendritic spines (blue), and postsynaptic densities (yellow) on the heads of each spine. (a) A single-synapse bouton associated with a thin spine; the translucent window reveals the numerous vesicles inside the presynaptic bouton. (b) Same spine as in A illustrating the position of the two docked vesicles at two different locations across from the yellow PSD. (c) The vesicles across from the PSD cluster in two distinct clumps that are separated by a blue ridge in the spine that contains a spinule (white arrow). (d) The segmented PSD of this large mushroom shaped spine is connected to the parent dendrite by the long thin neck at the right. (e) Reconstruction of a multiple synapse bouton (MSB) (purple) and its associated postsynaptic dendritic spines (blue) from different dendrites. The dendrite of the lower spine is also shown here. (f) The vesicles surround one end of a mitochondrion (yellow oblong structure located to the right of the cluster of purple vesicles). Calibration bars are for the two figures above them.

Table 1. Effect of synaptic cleft volume on the concentration of neurotransmitter or other molecules released from the synaptic vesicles

Identity	PSD area μm^3	Non-docked Vesicles Total No.	Non-docked Vesicle Volume μm^3 (10^{-5})	Synaptic Cleft Volume μm^3 (10^{-3})	Percent Concentration in Cleft	Docked Vesicles Total No.	Maximum Percent Concentration
Thin 1	0.070	210	3.0	0.7	4.3%	6	25.8%
Thin 2	0.070	241	2.8	0.7	4.0%	2	8.0%
Mushroom 1	0.100	529	2.6	0.5	5.2%	16	83.2%
Mushroom 2	0.150	459	2.0	1.3	1.5%	13	19.5%
Segmented PSD	0.420	1086	3.0	8.0	0.4%	36	14.4%
MSB 1, Thin	0.080	514	2.7	1.9	1.4%	11	15.4%
MSB 1, Stubby	0.060	—	2.7	1.8	1.5%	12	18.0%
MSB 2, Mushroom	0.120	492	3.0	1.6	1.9%	11	20.9%
MSB 2, Thin	0.085	—	3.0	N/A	N/A	2	N/A

The top 5 single-synapse boutons are identified by the shape of the spines synapsing with them. The top 4 spines had macular PSDs. The segmented PSD occurred on the large mushroom-shaped spine [Fig. 2 (c, d)]. The 2 MSBs each had 2 postsynaptic spines which are identified by their shapes. Vesicle volumes were computed as Vol = $4/3\ \pi r^3$, where r = the calculated diameter/2 and expressed as the mean ($\mu m^3 * 10^{-5}$) for each bouton. N/A, not available because the PSD was cut *en face*, thereby obscuring the region of the cleft. ND, Non-docked.

Graphics Laboratory at Children's Hospital, and three-dimensional reconstructions were obtained on the ICAR graphics workstation (ISG Technologies, Ontario, Canada). As indicated above, seven typical axonal boutons and their associated synaptic components were reconstructed.

Of this sample, four boutons each synapsed with a single dendritic spine. Two of the spines were of the thin shape category [e.g. Fig. 2(a,b)] and two were mushroom-shaped. All four had a continuous, macular-shaped PSD and the docked vesicles were distributed at various locations around the PSD, like the 2 docked vesicles which are on opposite sides of the PSD in Fig. 2(b) (purple spheres).

One bouton synapsed with a large mushroom-shaped spine that had a segmented PSD [Fig. 2(c, d)]. The vesicles in this presynaptic bouton formed two nearly distinct clusters over the main PSD segments that were separated by a ridge in the spine with a spinule in its center [Fig. 2(c), arrow]. Each of the segments of the PSD were irregularly shaped and had holes (perforations) in them [Fig. 2(d)]. The 36 docked vesicles were distributed across all segments of this PSD.

Two of the boutons each formed synapses with two postsynaptic dendritic spines, both of which had macular PSDs [e.g. Fig. 2(e, f)]. The vesicles in these boutons appeared to emanate from a continuous stream, however there was a lower density of vesicles in the center of the bouton where they surround one side of a mitochondrion [Fig. 2(f)]. These boutons are referred to as multiple synapse boutons (MSBs) (Sorra and Harris, 1993).

Dimensions of synaptic vesicles

Only those vesicles that were contained within the section were measured by placing a trace on the middle of their delimiting membrane. A total of 3531 non-docked vesicles were measured (Table 1). Gray profiles, which were likely to be the grazed edges of vesicles, were observed in the center of the bouton but they were not measured because the delimiting membrane was not present. In this way we avoided measuring incomplete vesicles and double counting of vesicles spanning more than one section. However, these precautions may also have resulted in somewhat lower counts of vesicles than what actually occur in the boutons. The perimeter of the traced membrane was compared to the projected area of the vesicles to determine whether they were spherical, where the shape parameter was computed from the (perimeter^2/4 π* area) and equals 1 for a perfect circle. For the non-docked vesicles this parameter ranged from 1.1 to 1.5; by way of contrast, the shape parameter ranged up to 9 or 10 for the elongated synaptic clefts. Thus, the spherical nature of the vesicles allowed us to use the formula for the area of a circle to estimate the diameter of each vesicle from the traced area ($d = 2*\sqrt{\text{area}/\pi}$). A frequency histogram of the computed diameters was plotted for each bouton (Fig. 3, solid lines). In all of the boutons, the non-docked vesicles averaged from 33 to 38 nm in diameter with an overall range of 20–66 nm.

A total of 109 docked vesicles were measured (Table 1). The number of docked vesicles ranged from 2 to 36 with larger PSDs having more docked vesicles. This estimate is probably low because we did not include the dark profiles at the active zones which might have been 'collapsed' vesicles. Most of the docked vesicles were either smaller than the non-docked vesicles or occurred at the lower end of the distribution, ranging in diameter from 23 to 49 nm (Fig. 3, dashed lines).

Percent concentration of vesicle contents in the synaptic cleft (Table 1)

Vesicle volumes were computed from the calculated diameters. The volume of the synaptic cleft occurring between the spine and presynaptic bouton was computed by multiplying its traced area times section thickness and adding across sections. Assuming free diffusion for glutamate and other small molecules released into the synaptic cleft, the percent concentration in the cleft was estimated by dividing the volumes of the non-docked vesicles by the volume of the synaptic cleft, and

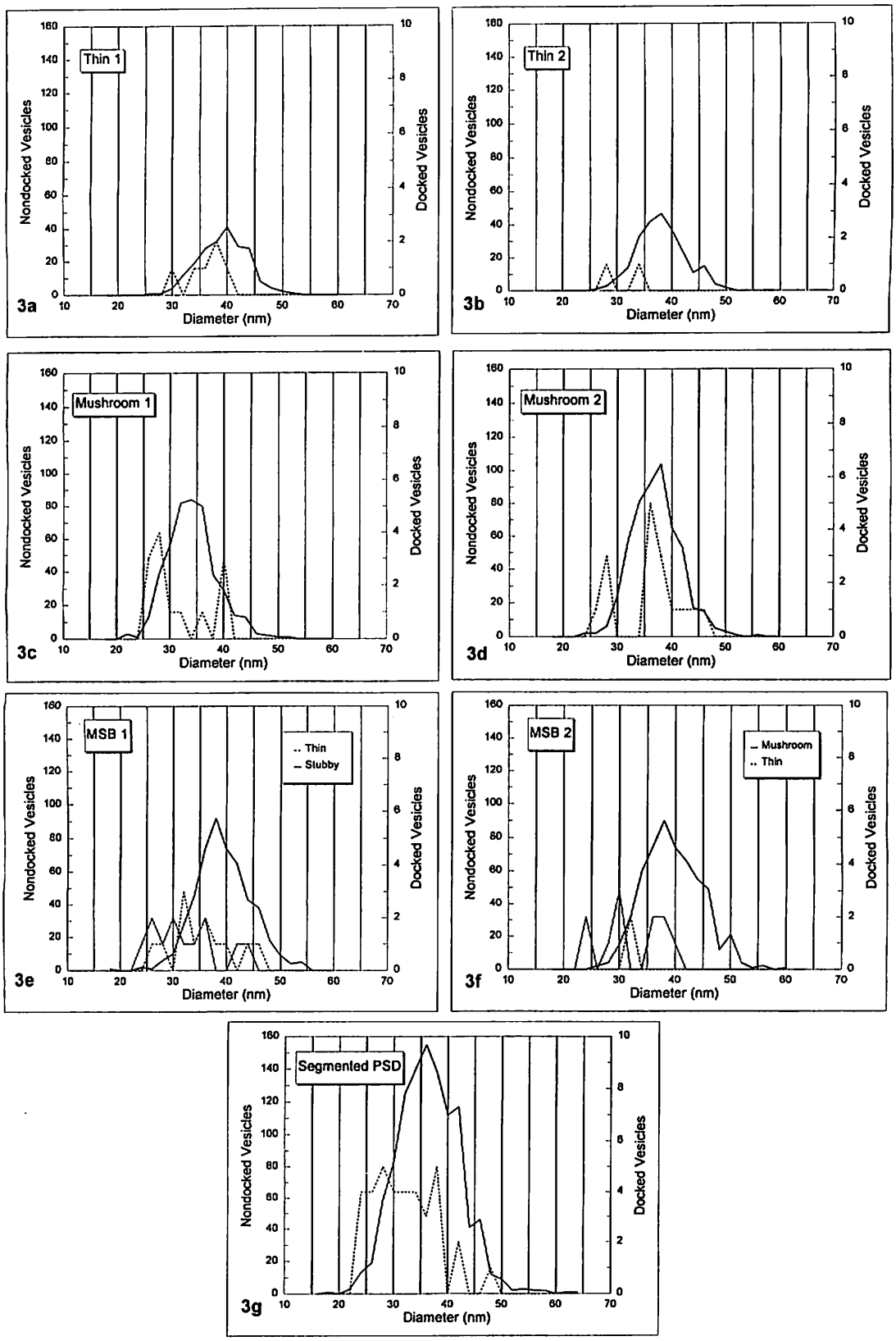

Fig. 3. Diameters of non-docked and docked vesicles in each of the seven reconstructed boutons. Each graph is for 1 of the boutons, solid lines are for the number of non-docked vesicles (left *y*-axis), and dashed lines are for the number of docked vesicles (right *y*-axis) at each diameter. In graphs (a)-(d) there was only one PSD associated with each bouton. In graphs (e) and (f) distributions for the two sets of docked vesicles, 1 for each PSD, are displayed with dashed or dotted lines and are indicated by the type of dendritic spine in each case. In graph (g) the solid line is for non-docked vesicles and the dashed line is for docked vesicles.

computing the mean percent for each bouton (Table 1). The non-docked vesicles were used for this estimate because many of the docked vesicles were smaller, which could indicate that they had released part of their contents or were in the process of re-uptake at the time of fixation. Based on the volumes alone, the concentration in the cleft would range from 0.4 to 5.2% of that in the non-docked vesicles. The maximum concentration would range from 8 to 83% if all of the docked vesicles were to release their contents simultaneously. The volume of the extracellular space adjoining each of the synaptic clefts ranged from 0.2 to 1.2 times the volume of the synaptic cleft, which could lead to further reductions in these concentrations depending on the time course of diffusion away from the cleft.

Relationship of synaptic vesicles to the dimensions of the PSD

The total area of each PSD was measured through serial sections using our standard methods (Harris *et al.*, 1992; Harris and Stevens, 1988, 1989). PSD areas ranged from 0.07 μm^2 on the thin spines to 0.42 μm^2 on the large mushroom spine with the segmented PSD (Table 1). As reported earlier, the total number of vesicles in the bouton increases with the size of the PSD (Harris and Stevens, 1988, 1989; Lisman and Harris, 1993). There were also more *docked* vesicles distributed around the larger PSDs raising the possibility of a higher probability of release as well as the possibility for multivesicular release to compensate for a greater dilution of neurotransmitter in the larger synaptic clefts of the bigger PSDs (Table 1).

Other characteristics of the presynaptic bouton

The presynaptic boutons ranged in volume from 0.12 to 0.43 μm^3. Two of the single-synapse boutons contained a single mitochondrion; one MSB contained one mitochondrion and the other MSB contained two mitochondria. The three remaining single-synapse boutons had no mitochondria, including the one on the segmented PSD. The axons connected to each of these three boutons could be traced for at least 1 μm along the constricted intervarcosity regions (<0.25 μm dia), but no mitochondria were found in these regions either.

Cisterns and tubes with smooth membranes were identified in all 7 boutons and could be components of the endosomal system. Coated vesicles or pits were observed in 3 of the boutons at the axonal membrane away from the presumed release site at the PSD. In two of the boutons there was some question about whether coated pits could be identified, and in two boutons no coated pits or vesicles were observed.

Astrocytic processes

Astrocytic processes were found adjacent to each of the seven boutons and/or their associated dendritic spines. Usually the astrocytic process did not surround the bouton, but rather formed a sheet on one side or produced several finger-like projections near to the spine head, around the spine neck, and at various points around the bouton (e.g. see Fig. 1).

DISCUSSION

The variation in number of docked vesicles ranged from 2 to 36 vesicles in proportion with synaptic size, and is consistent with physiological findings of a non-uniform probability of release at hippocampal synapses (Hessler *et al.*, 1993; Rosenmund *et al.*, 1993). The number of docked vesicles also coincides with recent estimates of the number of release sites and the 'readily releasable' pool of vesicles (Stevens and Tsujimoto, 1995; Ryan and Smith, 1995).

The dimensions of the vesicles show that the concentration of neurotransmitter released from a single synaptic vesicle could be from 0.4 to 5.2% of its original concentration. Current evidence suggests that the concentration of glutamate in a single synaptic vesicle ranges from 60 to 210 mM (Nicholls and Attwell, 1990; Burger *et al.*, 1989; Riveros *et al.*, 1986). Based on our volumetric measurements, the concentration of glutamate in the synaptic cleft could approach 0.24–11 mM even after the release of a single vesicle. Of course, if multivesicular release were to occur, then the concentration in the cleft would be even higher. Recent measurements suggest that postsynaptic receptors at hippocampal synapses will be saturated when glutamate reaches 1.1 mM peak concentration (Clements *et al.*, 1992), thus these measurements support the hypothesis that the postsynaptic receptors will be saturated with glutamate during each event, even at large synapses (Clements *et al.*, 1992; Faber *et al.*, 1992; Redman, 1990; Jack *et al.*, 1994).

Several sources of variation could account for the distribution of vesicle dimensions presented in this report. These sources include (but may not be limited to), (1) the true variation in vesicle sizes depending on their functional state, (2) whether docked vesicles release all or only part of their contents during each synaptic event, (3) whether endocytosis occurs at the same site as exocytosis, and (4) the effect of variability in the placement of traces on the vesicular membrane and the synaptic cleft during the reconstructions. Section thickness is unlikely to be a source of variation in the measured vesicle volumes because we only measured vesicles for which the delimiting edges of the membrane were visible in a single section and then computed the volumes based on the projected areas of the essentially spherical vesicles. Fixation and processing conditions do not account for the range in variation among these vesicles because all of the boutons were obtained from a single hippocampus; however, these conditions may have altered the absolute dimensions in unknown ways (see below).

There was a remarkable similarity in the distributions of non-docked vesicle diameters attesting to their relative

uniformity across boutons. This uniformity in size distributions is especially apparent for particular spine types and PSD sizes, such that, the overall distributions for the two thin spines are identical and similarly for the two mushroom spines, and the two MSBs. On average the non-docked vesicle diameters ranging from 33 to 38 nm, which are comparable to other measurements from aldehyde fixed hippocampus (Bekkers *et al.*, 1990) and cerebellum (Palay and Chan-Palay, 1974), however they are somewhat smaller (about 7 nm in diameter) than previously reported for glutamatergic vesicles in the rapid-frozen anteroventrocochlear nucleus (Tatsuoka and Reese, 1989). Factors that could have contributed to these differences in measured dimensions of vesicle size include differences across brain regions, limited shrinkage during aldehyde fixation, rounding and swelling of vesicles due to subtle ice crystal formation during rapid freezing, or exactly where the diameters and/or delimiting membrane traces were placed on the vesicular membrane.

Coated vesicles and endosomes were observed at the opposite side of the axonal bouton, suggesting that this route for vesicular recycling is available at these hippocampal synapses (Maycox *et al.*, 1992; Miller and Heuser, 1984). The occurrence of smaller vesicles in the docked position may suggest 'incomplete' release events, (Neher, 1993) or re-uptake at the same site as release (Ceccarelli and Hurlbutt, 1980). Specific labeling at the EM level will be needed to discern whether one or both of these routes of SV recycling occur at hippocampal CA1 synapses. The rare occurrence of coated vesicles in these boutons suggests that turnover may be quick such that only a few are captured during conventional perfusion fixation. Alternatively, these boutons could have been in a resting state at the time of fixation (e.g. due to anesthesia prior to perfusion), and therefore, the large population of non-docked vesicles would reflect a quiet steady state.

It was curious that not all of the boutons had mitochondria in them and no mitochondria were found in the adjoining intervaricosity regions of their axons. In fact, the largest bouton with the most vesicles had no mitochondria. This finding is perplexing in light of the known requirements for ATP in several steps of the SV cycle (Sudhof, 1995). One possibility is that local areas of anaerobic glycolysis occur in the boutons (Borowsky and Collins, 1989). Another possibility is that the mitochondria migrate rapidly between boutons and along the axons such that sufficient ATP is produced and diffused throughout the axoplasm to sustain ongoing synaptic activity. Finally, it is possible that the neighboring astrocytic processes supply ATP via an extracellular route. Further experimentation will be needed to determine whether the absence of mitochondria in some of the boutons is a signature of differences in functional state.

These are some of the first measurements of the sizes, numbers and locations of synaptic vesicles throughout completely reconstructed axonal boutons in the hippocampal area CA1, a brain region that has been extensively evaluated for its role in synaptic plasticity. Recent physiological studies implicate changes in vesicle turnover and release in long-term potentiation (LTP) at individual hippocampal synapses (Arancio *et al.*, 1995; Malgaroli *et al.*, 1995). Of particular interest will be to know how the anatomical signatures of the different phases of the SV cycle are affected by enduring changes in synaptic efficacy, such as LTP.

Acknowledgements—We thank Robert Malinow, Heinrique Von Gersdorff and Max Snodderly for their helpful suggestions. P. Sultan was an undergraduate student in the Department of Biology at Harvard University and some of this work appeared in his honors thesis; he is currently at Cornell University Medical College, New York. This work is supported by NIH-NINDS No. NS21184 and by the MR Center Grant No. P30-HD18655 from NICHD.

REFERENCES

Arancio O., Kandel E. R. and Hawkins R. D. (1995) Activity-dependent long-term enhancement of transmitter release by presynaptic 3, 5-cyclic GMP in clutured hippocampal neurons. *Nature* **376:** 74–80.

Bekkers, Richerson G. B. and Stevens C. F. (1990) Origin of variability in quantal size in cultured hippocampal neurons and hippocampal slices. *Proc. Natn. Acad. Sci. U.S.A.* **87:** 5359–5362.

Betz W. J. and Bewick G. S. (1992) Optical analysis of synaptic vesicle recycling at the frog neuromuscular junction. *Science* **255:** 200–203.

Borowsky I. W. and Collins R. C. (1989) Metabolic anatomy of brain: a comparison of regional capillary density, glucose metabolism, and enzyme activities. *J. Comp. Neur.* **288:** 401–413.

Burger P. M., Mehl E., Cameron P. L., Maycox P. R., Baumert M., Lottspeich F., De Camilli P. and Jahn R. (1989) Synaptic vesicles immunoisolated from rat cerebral cortex contain high levels of glutamate. *Neuron* **3:** 715–720. (Abstract)

Ceccarelli B. and Hurlbutt W. P. (1980) Vesicle hypothesis of the release of quanta of acetylcholine. *Physiol. Rev.* **60:** 396–441.

Clements J. D., Lester R. A. J., Tong G., Jahr C. E. and Westbrook G. L. (1992) The time course of glutamate in the synaptic cleft. *Science* **258:** 1498–1501.

Faber D. S., Young W. S., Legendre P. and Korn H. (1992) Intrinsic quantal variability due to stochastic properties of receptor transmitter interactions. *Science* **258:** 1494–1498.

Harris K. M., Jensen F. E. and Tsao B. (1992) Three-dimensional structure of dendritic spines and synapses in rat hippocampus (CA1) at postnatal day 15 and adult ages: implications for the maturation of synaptic physiology and long-term potentiation. *J. Neurosci.* **12:** 2685–2705.

Harris K. M. and Stevens J. K. (1988) Dendritic spines of rat cerebellar Purkinje cells: serial electron microscopy with reference to their biophysical characteristics. *J. Neurosci.* **8:** 4455–4469.

Harris K. M. and Stevens J. K. (1989) Dendritic spines of CA1 pyramidal cells in the rat hippocampus: serial electron

microscopy with reference to their biophysical characteristics. *J. Neurosci.* **9:** 2982–2997.

Hessler N. A., Shirke A. M. and Malinow R. (1993) The probability of transmitter release at a mammalian central synapse. *Nature* **366:** 569–572.

Heuser J. E. and Reese T. S. (1973) Evidence for recycling of synaptic vesicle membrane during transmitter release at the frog neuromuscular junction. *J. Cell Biol.* **57:** 315–344. (Abstract)

Jack J. J. B., Larkman A. U., Major G. and Stratford K. J. (1994) Quantal analysis of the synaptic excitation of CA1 hippocampal pyramidal cells. In: *Molecular and Cellular Mechanisms of Neurotransmitter Release* (Stjarne L., Greengard P., Grillner S., Hokfelt T., Ottoson D., Eds), pp. 275–299. Raven Press, Ltd, New York.

Lisman J. and Harris K. M. (1993) Quantal analysis and synaptic anatomy—integrating two views of hippocampal plasticity. *Trends Neurosci.* **16:** 141–147.

Malgaroli A., Ting A. E., Wendland B., Bergamaschi A., Villa A., Tsien R. W. and Scheller R. H. (1995) Presynaptic component of long-term potentiation visualized at individual hippocampal synapses. *Science* **268:** 1624–1628.

Maycox P. R., Link E., Reetz A., Morris S. A. and Jahn R. (1992) Clathrin-coated vesicles in nervous tissue are involved primarily in synaptic vesicle recycling. *J. Cell. Biol.* **118:** 1379–1388.

Miller T. M. and Heuser J. E. (1984) Endocytosis of synaptic vesicle membrane at the frog neuromuscular junction. *J. Cell. Biol.* **98:** 685–698.

Neher E. (1993) Secretion without full fusion. *Nature* **363:** 497–498.

Nicholls D. and Attwell D. (1990) The release and uptake of excitatory amino acids. *Trends Pharm. Sci.* **11:** 462–468.

Palay S. L. and Chan-Palay V. (1974) *Cerebellar cortex: cytology and organization*. Springer-Verlag, New York.

Peters A., Palay S. L. and Webster Hd. (1991) *The fine structure of the nervous system: The neurons and supporting cells*. W. B. Saunders, Co., Toronto.

Redman S. (1990) Quantal analysis of synaptic potentials in neurons of the central nervous system. *Physiol. Rev.* **70:** 165–198.

Riveros N., Fiedler J., Lagos N., Munoz C. and Orrego F. (1986) Glutamate in rat brain cortex synaptic vesicles: influence of the vesicle isolation procedure. *Brain Res* **386:** 405–408 (Abstract).

Rosenmund C., Clements J. D. and Westbrook G. L. (1993) Nonuniform probability of glutamate release at a hippocampal synapse. *Science* **262:** 754–757.

Ryan T. A., Reuter H., Wendland B., Schweizer F. E., Tsien R. W. and Smith S. J. (1993) The kinetics of synaptic vesicle recycling measured at single presynaptic boutons. *Neuron* **11:** 713–724.

Ryan T. A. and Smith S. J. (1995) Vesicle pool mobilization during action potential firing at hippocampal synapses. *Neuron* **14:** 983–989.

Schwartz J. H. (1992) Synaptic Vesicles. In: *Principles of Neural Science* (Anonymous) pp. 225–234. Elsevier, New York.

Sorra K. E. and Harris K. M. (1993) Occurrence and three-dimensional structure of multiple synapses between individual radiatum axons and their target pyramidal cells in hippocampal area CA1. *J Neurosci.* **13:** 3736–3748.

Stevens C. F. and Tsujimoto T. (1995) Estimates for the pool size of releasable quanta at a single central synapse and for the time required to refill the pool. *Proc. Natn. Acad. Sci. U.S.A.* **92:** 846–849.

Sudhof T. C. (1995) The synaptic vesicle cycle: a cascade of protein-protein interactions. *Nature* **375:** 645–653.

Tatsuoka H. and Reese T. S. (1989) New structural features of synapses in the anteroventral cochlear nucleus prepared by direct freezing and freeze-substitution. *J. Comp. Neur.* **290:** 343–357.